Check for updates

Recyclization of morpholinochromonylidene–thiazolidinone using nucleophiles: facile synthesis, cytotoxic evaluation, apoptosis, cell cycle and molecular docking studies of a novel series of azole, azine, azepine and pyran derivatives†

Tarik E. Ali, [iD] *[a] Mohammed A. Assiri,[a] Maha N. Alqahtani,[a] Ali. A. Shati,[b] Mohammad. Y. Alfaifi[b] and Serag. E. I. Elbehairi[b]

A convenient synthetic approach for construction of a novel series of substituted azoles, azines, azepines and pyrans clubbed with a morpholinothiazolidinone hybrid was achieved. The methodology depended on ring-opening and ring-closure (RORC) of chromone ring in 2-(morpholinoimino)-5-[(4-oxo-4*H*-chromen-3-yl)methylene]-3-phenylthiazolidin-4-one (**3**) through its reaction with a series of nitrogen and carbon nucleophiles under mild reaction conditions. The cytotoxic effects of all products were evaluated against three cancerous cell lines (MCF-7, HepG-2 and SKOV-3) by the standard SRB method. Fortunately, the products **7**, **11**, **12**, **15**, **19**, **22**, **26** and **28** were found to be the most active against all cancer cell lines, comparable to doxorubicin. Apoptosis was determined using flow cytometry along with cell cycle analysis and supported by molecular docking. The products **7**, **11**, **12**, **15**, **19**, **22**, **26** and **28** induced a significant early-and late-apoptotic effect against all tumor cells. In addition, these products preferred to arrest all cancer cells in the G1 and G2 phases. Finally, molecular docking was attempted to investigate the binding mode of products **12** and **22** with p53-MDM2 protein receptor.

1. Introduction

Cancer has become the most prominent life-threatening disease, presenting a serious health challenge worldwide. Despite considerable research in cancer treatment, there is still a continuing need for novel cancer treatments.[1] The development of multiple drug resistance to antitumor drugs is a major problem in chemotherapy. Hence, research for the invention of novel agents for treating cancer is of prime importance.[2]

Combination of morpholine and thiazolidinone rings in one molecular structure has been proved for its potency as antimicrobial,[3–6] anticancer,[6] antioxidant,[7] antihistaminic and anticholinergic agents[8] as well as a neuroprotective agent against cerebral ischemia reperfusion.[9] On the other hand, chromone compounds have long gained interest as highly reactive molecules that can be used as precursors in the synthesis of a wide variety of heterocycles. They possess important chemical properties due to the presence of two active

electrophilic centers at the C–2 and C=O$_{pyrone}$ groups. Therefore, chromone rings can react with nitrogen and carbon nucleophiles, that begin by ring opening at the unsubstituted C–2 then recyclization through condensation with the pyrone group forming a variety of heterocycles.[10,11] Starting from the previous facts and results that based on our successful trials research in the preparation of antiproliferative agents,[12–15] we aim here to construct a novel series of oxygen and nitrogen heterocycles linked with morpholinothiazolidinone moiety to investigate their cytotoxic effects. The methodology depended on ring opening and ring closure (RORC) of the chromone ring in 2-(morpholinoimino)-5-[(4-oxo-4*H*-chromen-3-yl)methylene]-3-phenyl-thiazolidin-4-one (**3**) through its reaction with some nitrogen and carbon nucleophiles under mild conditions.

2. Results and discussion

Construction of 2-(morpholinoimino)-5-[(4-oxo-4*H*-chromen-3-yl)methylene]-3-phenyl-thiazolidin-4-one (**3**) as the starting material, was achieved through one-pot three components reaction of 1-morpholino-3-phenylthiourea (**1**), ethyl bromoacetate and 3-formyl-chromone (**2**) in ethanol in the presence of anhydrous sodium acetate (Scheme 1, see ESI section†).
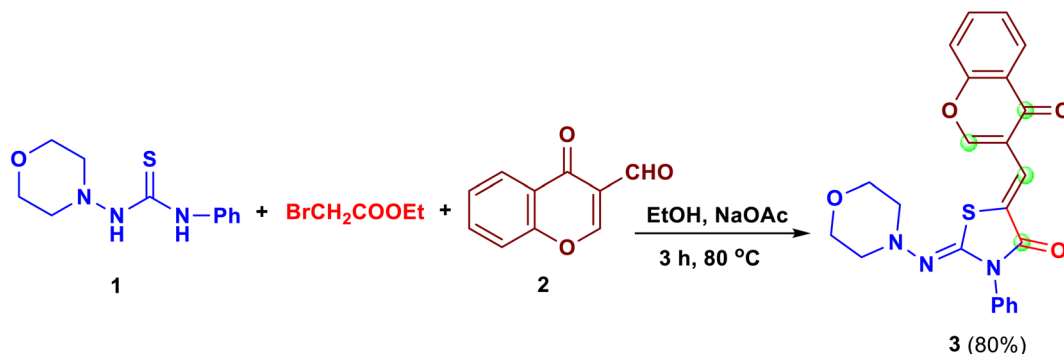
The substrate **3** is a very active starting material toward nitrogen and carbon nucleophiles. This substrate has four

[a]Department of Chemistry, Faculty of Science, King Khalid University, Abha, 61421 Saudi Arabia. E-mail: tarik_elsayed1975@yahoo.com; tismail@kku.edu.sa

[b]Department of Biology, Faculty of Science, King Khalid University, Abha, 61421 Saudi Arabia

Scheme 1 Synthesis of the starting material **3**.

possible electrophilic centers at the C–2$_{chromone}$, C=O$_{chromone}$, =CH$_{exocyclic}$ and C=O$_{thiazole}$ groups as two cyclic α,β-unsaturated ketones.[16] Logically, the C–2$_{chromone}$ has electrophilic character more than =CH$_{exocyclic}$ due to electronegativity of oxygen atom. The present work aims to study the ring opening and recyclization reactions of the starting material **3** toward a variety of nitrogen and carbon nucleophiles to synthesize a novel series of oxygen and nitrogen heterocycles linked with morpholinothiazolidinone moiety.

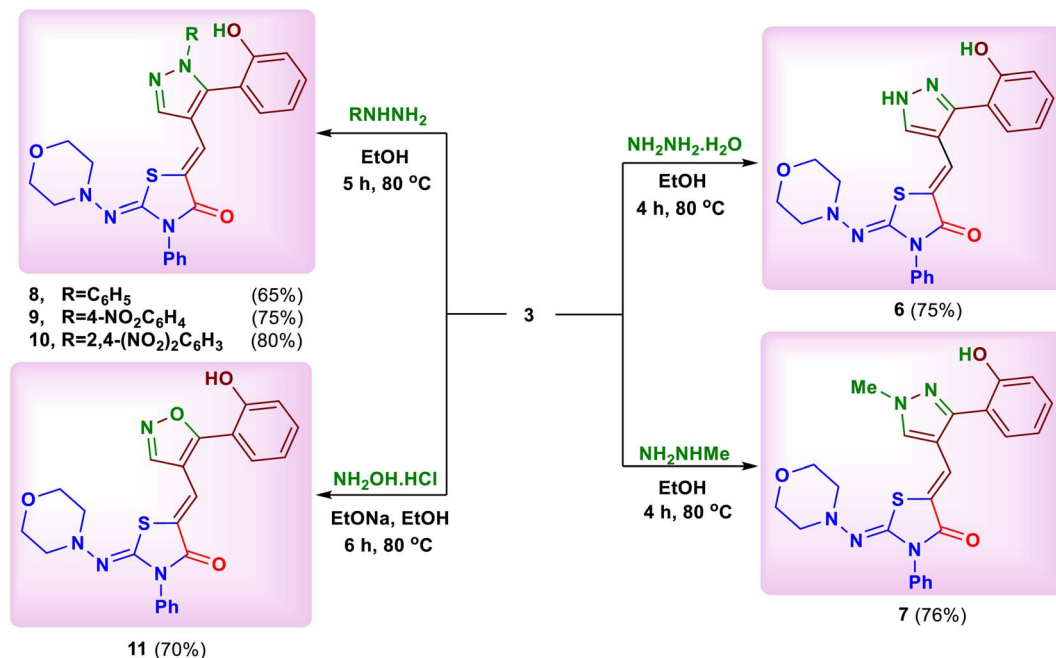### 2.1. Reaction with nitrogen nucleophiles

Heating of the substrate **3** with some selected amines such as 4-aminomorpholine and morpholine in absolute ethanol afforded 5-[2-(2-hydroxybenzoyl)-3-(morpholinoamino) allylidene]-2-(morpholinoimino)-3-phenylthiazolidin-4-one (**4**) and 5-[2-(2-

hydroxybenzoyl)-3-morpholino-allylidene]-2-(morpholinoimino)-3-phenylthiazolidin-4-one (**5**), respectively (Scheme 2).[17] The reaction started through a nucleophilic attack at C–2 position of chromone ring by ring opening to yield these products.

Next, the chemical reactivity of substrate **3** was studied toward nitrogen 1,2-*bi*-nucleophiles. Thus, treatment of compound **3** with some hydrazines namely, hydrazine hydrate, methylhydrazine, phenylhydrazine, 4-nitrophenylhydrazine and 2,4-dinitrophenylhydrazine in absolute ethanol under reflux gave the corresponding pyrazole derivatives **6–10**, respectively (Scheme 3).[16] Similarly, the oxazole derivative **11** was obtained by reaction of compound **3** with hydroxylamine hydrochloride in ethanolic sodium ethoxide (Scheme 3).[18] The plausible mechanism for formation of these azoles suggested a nucleophilic attack by NH$_2$ or NH-Me group at C–2 of

Scheme 2 Reaction of the substrate **3** with 4-aminomorpholine and morpholine.

Scheme 3 Reaction of the substrate **3** with nitrogen 1,2-*bi*-nucleophiles.

chromone ring with ring opening followed by closure occurred by another nucleophilic attack of XH group (X = NH, NR, O) on the C=O$_{benzoyl}$ with removal of water molecule.[16]
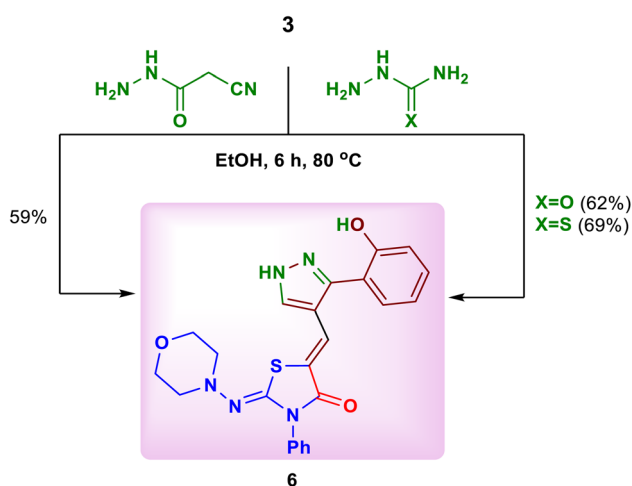
Interestingly, the reaction of the substrate **3** with some hydrazides such as semicarbazide, thiosemicarbazide and cyanoacetohydrazide in absolute ethanol or ethanolic sodium ethoxide, was studied. In all cases, the previous product, 5-{[3-(2-hydroxyphenyl)-1*H*-pyrazol-4-yl] methylene}-2-(morpholinoimino)-3-phenylthiazolidin-4-one (**6**) was isolated (Scheme 4).

Based on the above mentioned results, the work was extended to study the behavior of nitrogen 1,3-*bi*-nucleophiles towards the substrate **3**. Thus, the reaction of compound **3** with

urea, thiourea, selenourea and guanidine carbonate in ethanolic sodium ethoxide afforded the corresponding 5-{[4-(2-hydroxyphenyl)-2-oxo(thioxo)(selenoxo)-1,2-dihydropyrimidin-5-yl] methylene}-2-(morpholinoimino)-3-phenylthiazolidin-4-ones **12–14** and 5-{[2-amino-4-(2-hydroxyphenyl)pyrimidin-5-yl] methylene}-2-(morpholinoimino)-3-phenylthiazolidin-4-one (**15**), respectively (Scheme 5).[19]
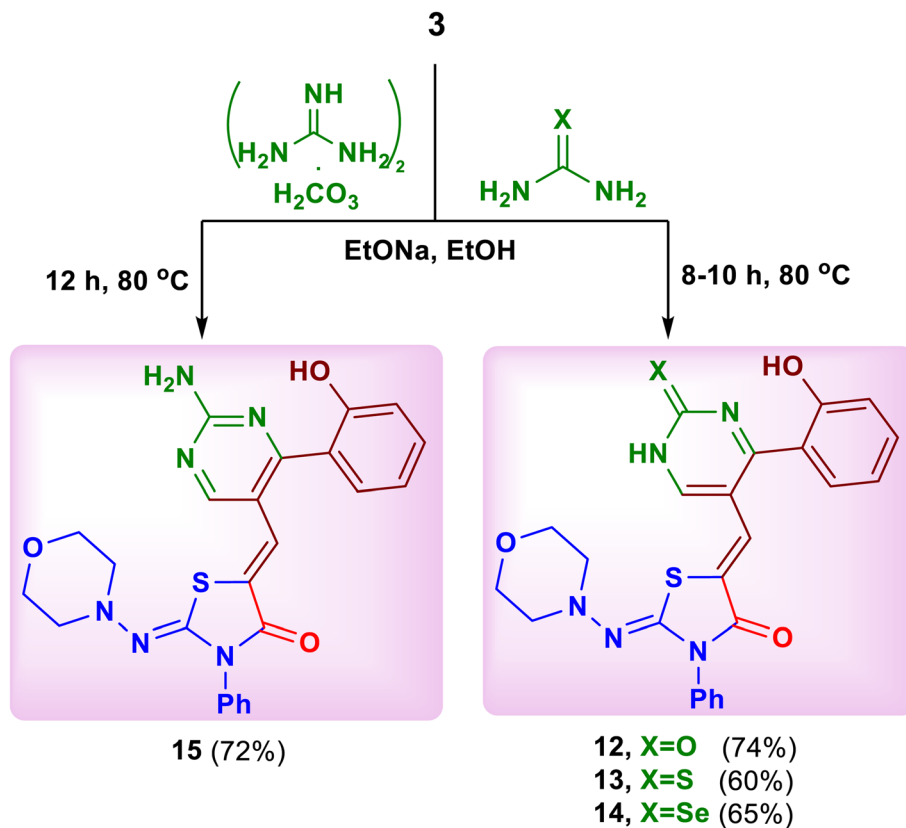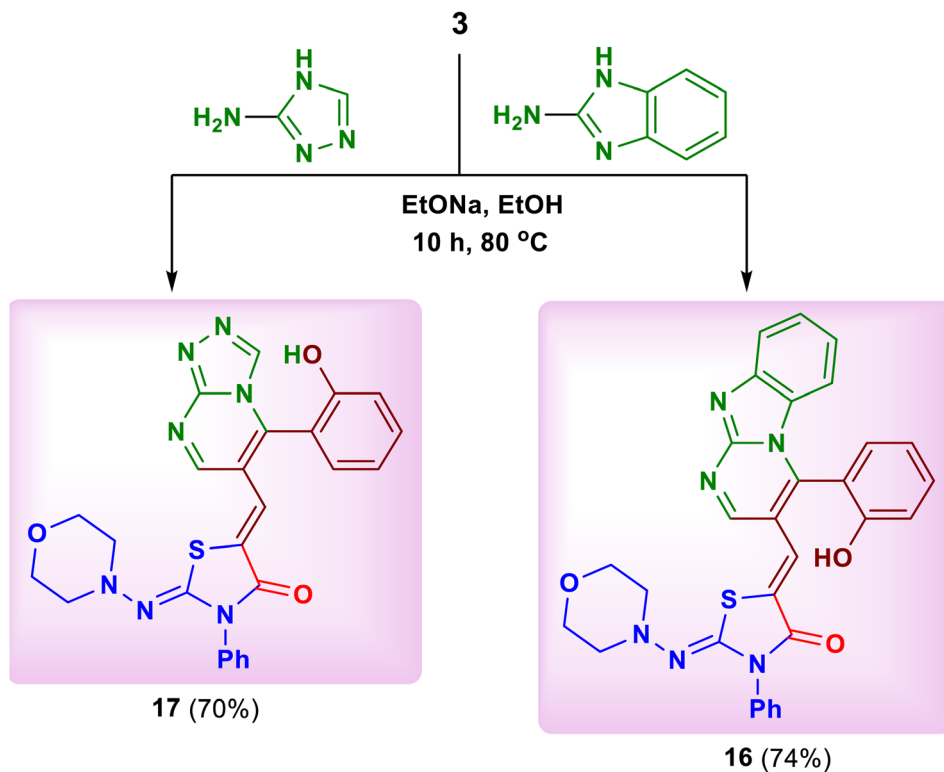
Similarly, the reaction of 2-aminobenzimidazole and 3-amino-4*H*-[1,2,4]-triazole as cyclic nitrogen 1,3-*bi*-nucleophiles with the substrate **3** under the previous reaction conditions led to the formation of 5-{[4-(2-hydroxyphenyl)benzo[4,5]imidazo[1,2-*a*]pyrimidin-3-yl]methylene}-2-(morpholinoimino)-3-phenylthiazolidin-4-one (**16**) and 5-{[5-(2-hydroxy-phenyl)-[1,2,4 triazolo[4,3-*a*]pyrimidin-6-yl]methylene}-2-(morpholinoimino)-3-phenylthiazolidin-4-one (**17**), respectively (Scheme 6).[20] The spectral data of both products **16** and **17** confirmed their structures (see ESI†).
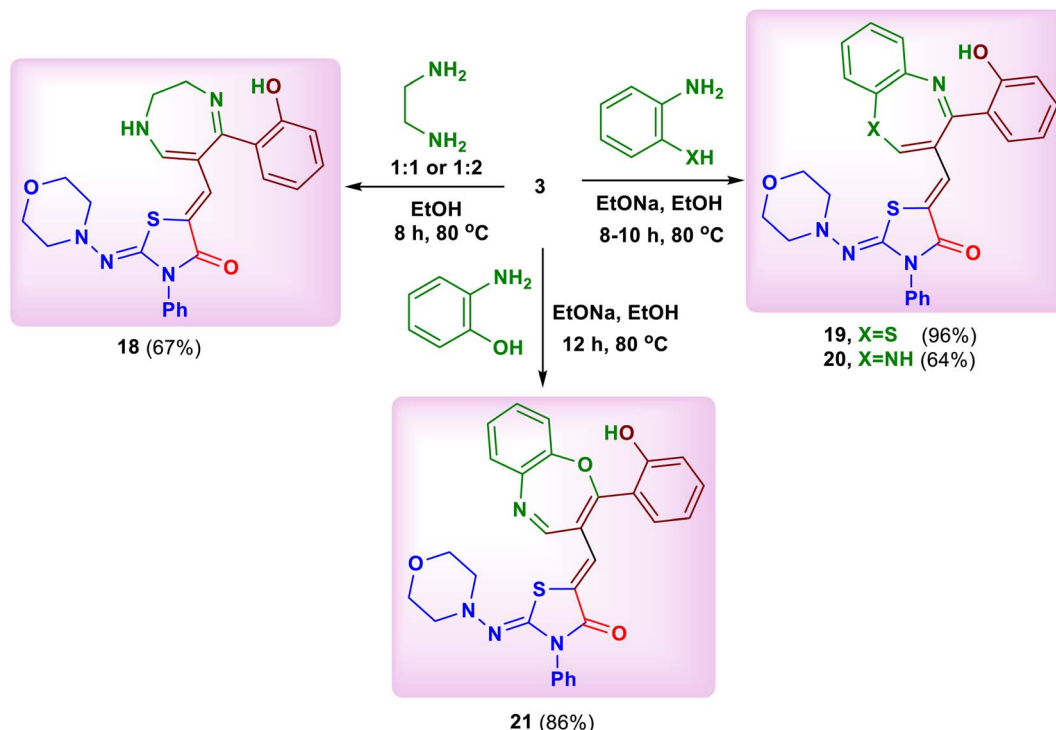
Seven-membered heterocycles with two heteroatoms are known to possess several biological activities.[21–23] The present study was extended to investigate the chemical reactivity of the substrate **3** with classical nitrogen 1,4-*bi*-nucleophiles to construct seven-membered heterocyclic systems clubbed with morpholinothiazolidinone moiety. Thus, treatment of compound **3** with ethylenediamine in 1 : 1 or 1 : 2 molar ratio in ethanol led to formation of 5-[(5-(2-hydroxyphenyl)-2,3-dihydro-1*H*-1,4-diazepin-6-yl)methylene]-2-(morpholinoimino)-3-phenylthiazolidin-4-one (**18**) (Scheme 7). In the same way, heating of the substrate **3** with 2-aminothiophenol, 1,2-phenylenediamine and 2-aminophenol in ethanolic sodium ethoxide yielded the corresponding benzothiazepine, benzodiazepine and benzoxazepine derivatives **19–21**, respectively (Scheme 7).
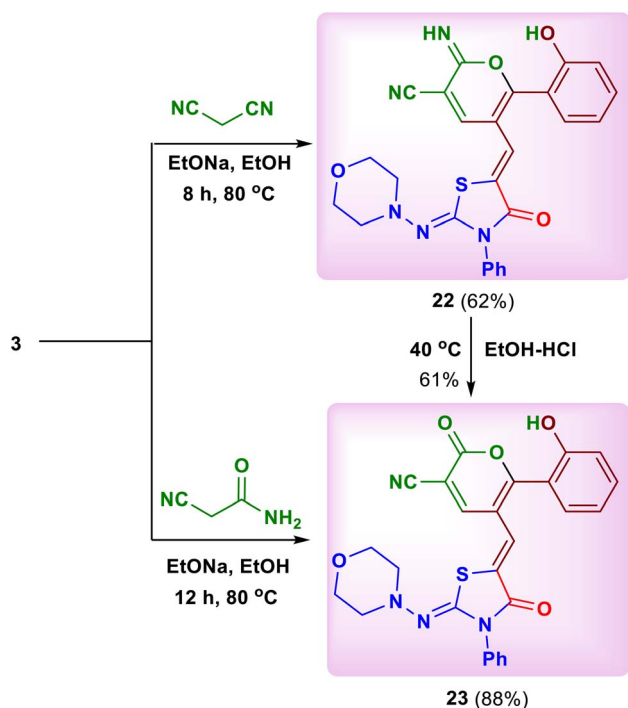

Scheme 4 Reaction of the substrate **3** with some hydrazides.

3

Scheme 5 Reaction of the substrate **3** with urea, thiourea, selenourea and guanidine carbonate.

3

Scheme 6 Reaction of the substrate **3** with 2-aminobenzimidazole and 3-amino-4*H*-1,2,4-triazole.

Scheme 7 Reaction of the substrate **3** with ethylenediamine, 2-aminothiophenol, 1,2-phenylenediamine and 2-aminophenol.

Scheme 8 Reaction of the substrate **3** with malononitrile and cyanoacetamide.
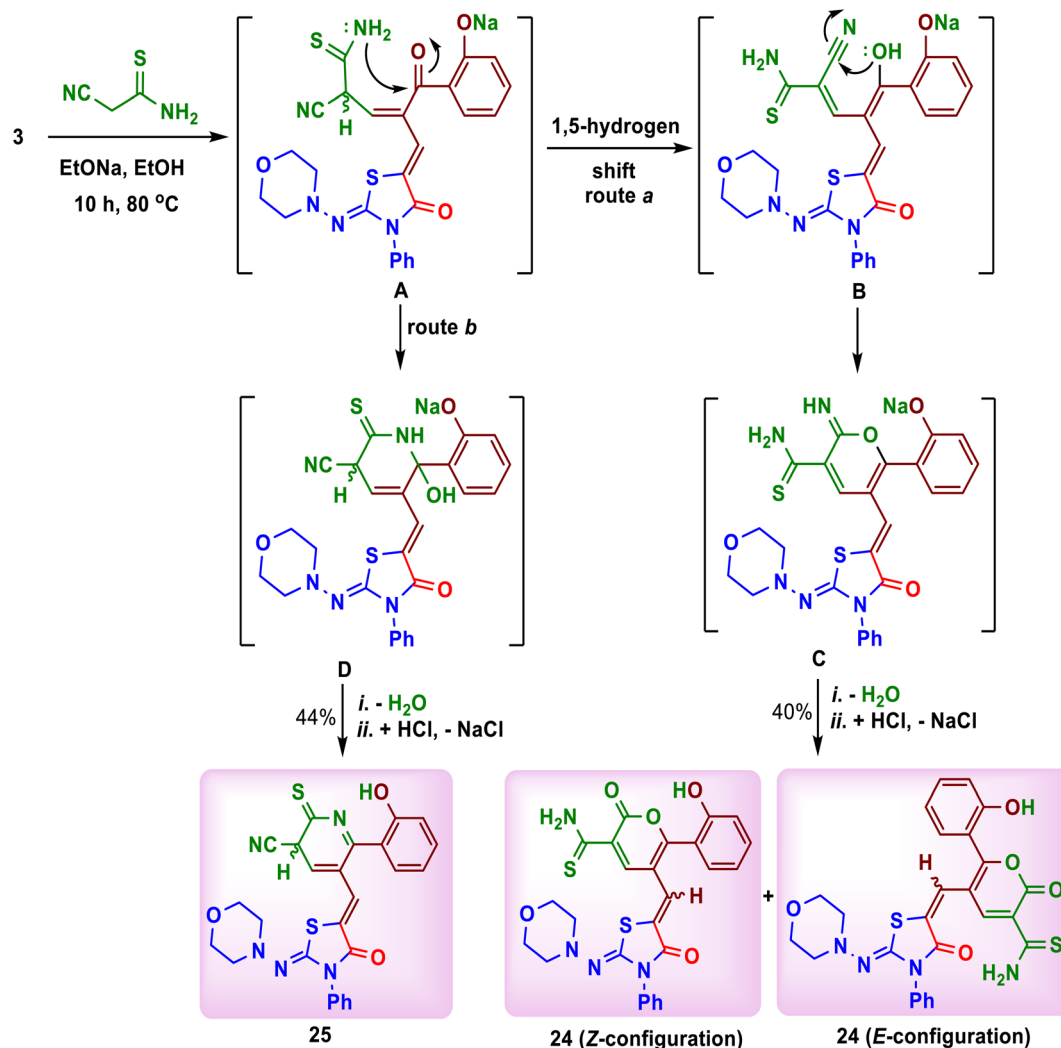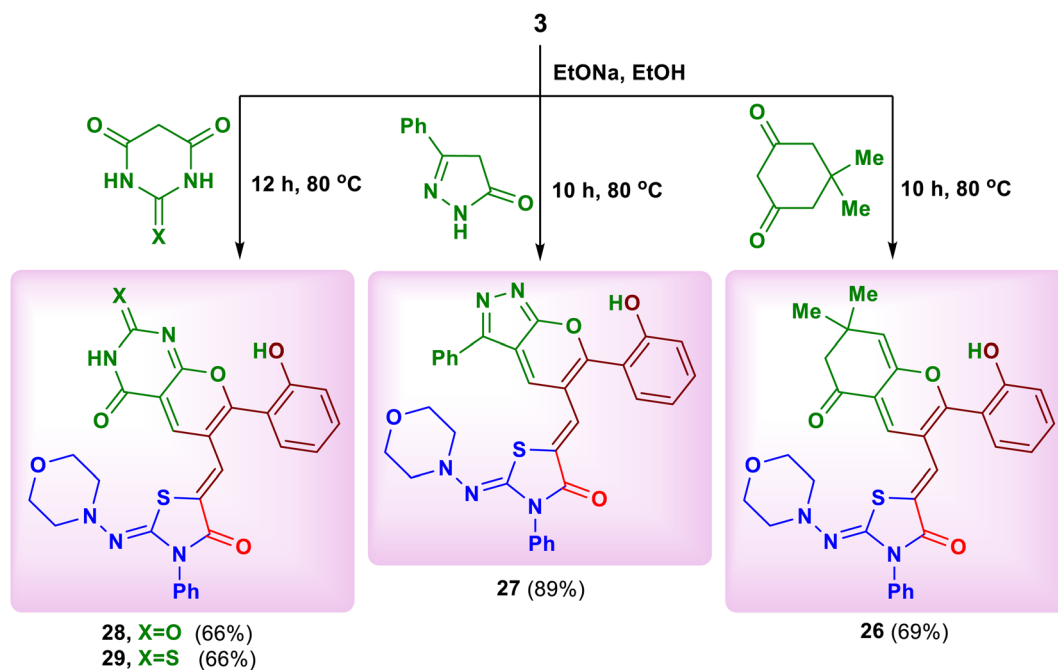
2.2. Reaction with carbon nucleophiles

We also studied the effect of acyclic and cyclic carbon nucleophiles which can construct various novel pyran and pyridine
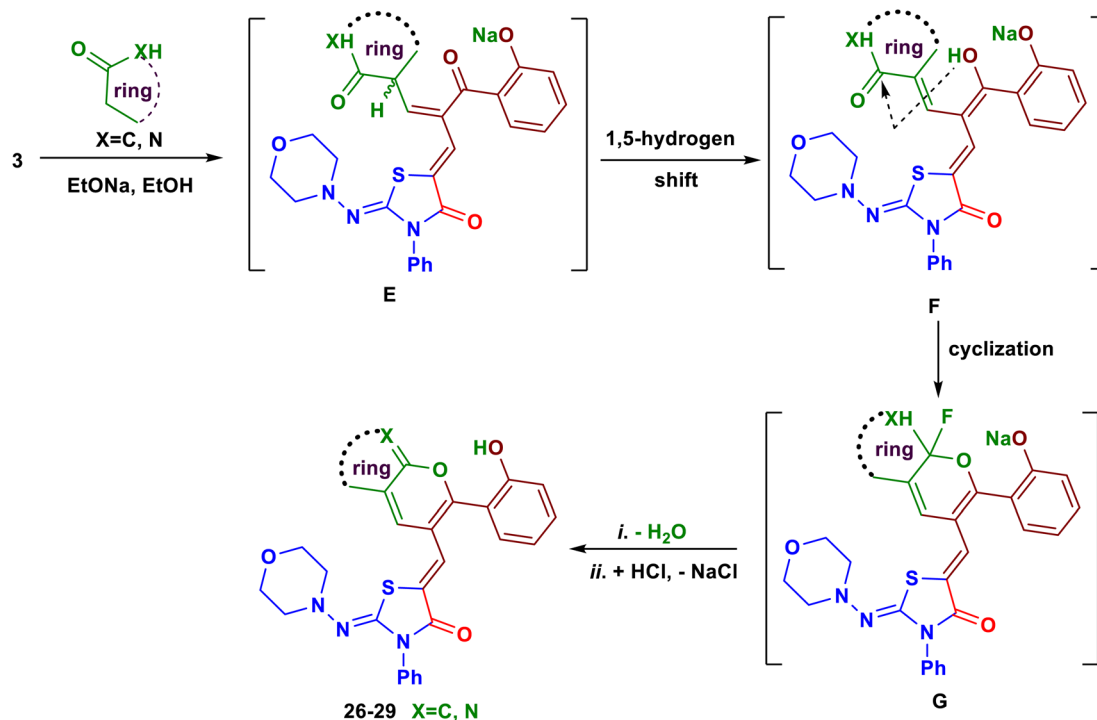
compounds in an efficient and economical way. Thus, a simple treatment of 2-(morpholinoimino)-5-[(4-oxo-4H-chromen-3-yl) methylene]-3-phenylthiazolidin-4-one (**3**) with each one of acyclic carbon nucleophiles, namely malononitrile and cyanoacetamide in ethanol in the presence of sodium ethoxide at 80 °C afforded 6-(2-hydroxyphenyl)-2-imino-5-{[2-(morpholinoimino)-4-oxo-3-phenylthiazolidin-5-ylidene] methyl}-2H-pyran-3-carbonitrile (**22**) (Scheme 8) and 6-(2-hydroxyphenyl)-5-{[2-(morphol-inoimino)-4-oxo-3-phenyl-thiazolidin-5-ylidene]methyl}-2-oxo-2H-pyran-3-carbonitrile (**23**), respectively (Scheme 8).[24] In addition, the product **23** was also obtained by acidic hydrolysis of compound **22** in ethanol (Scheme 8). The ^{1}H-NMR spectrum of **22** displayed specific singlets at δ 8.22 (H–4$_{pyran}$), 10.11 (NH) and 9.87 (OH) ppm, while compound **23** displayed the =CH and H–4$_{pyrone}$ protons as singlets at δ 8.17 and 8.86 ppm, respectively. Consequently, the ^{13}C-NMR spectrum of **22** confirmed the existence of C–2 and C≡N atoms of the pyran ring at δ 161.9 and 114.3 ppm, respectively. In addition, there are two characteristic signals in compound **23** at δ 114.1 and 172.6 ppm due to C≡N and C= O$_{pyrone}$, respectively.

The interesting point in this work was the reaction of substrate **3** with cyanothioacetamide in ethanolic sodium ethoxide. The reaction did not form a similar product to compound **23**, but it afforded 6-(2-hydroxyphenyl)-5-(Z/E)-{[2-oxo-2H-pyran-3-carbothioamido-5-yl]methylene}-2-(morpholinoimino)-3-phenylthiazolidin-4-one (**24**) as red crystals on heating after 2 hours (Scheme 9). In addition, cooling of the filtrate of the reaction mixture and its neutralization with diluted hydrochloric acid, yielded 6-(2-hydroxyphenyl)-5-{[3-cyano-2-thioxo-

Scheme 9 Reaction of the substrate **3** with cyanothioacetamide.

Scheme 10 Reaction of the substrate **3** with some cyclic carbon nucleophiles.

Scheme 11 The possible mechanism for reaction of the substrate **3** with some cyclic carbon nucleophiles.

2,3-dihydropyridine-5-yl]methylene}-2-(morpholinoimino)-3-phenylthiazolidin-4-one (**25**) as orange crystals (Scheme 9). The formation of both products **24** and **25** was explained as depicted in Scheme 9. Interestingly, the ^{1}H and ^{13}C-NMR spectra of compound **24** displayed duplication of the expected protons and carbons. This may be due to the presence of the *Z*- and *E*-configurations of the product **24** in ratio 1 : 1.[25] The H–4$_{pyrone}$ and OH protons appeared as singlets at δ 8.08, 8.24 and 8.44, 8.89 ppm, respectively, while NH$_2$ and =CH protons were found in the aromatic region between δ 7.37 and 7.58 ppm. Further, the ^{13}C-NMR spectrum of compound **24** supported the presence of the =CH$_{exocyclic}$ (127.3, 127.5), C–4$_{pyran}$ (139.1, 139.9), C=O$_{pyrone}$ (161.2, 161.9) and C=S$_{thioamide}$ (180.5, 180.9) ppm, respectively. On the other hand, the ^{1}H-NMR spectrum of compound **25** displayed the H–3 and H–4 protons of pyridine ring as two doublets at δ 6.11 (J = 3.2 Hz) and 8.28 (J = 3.2 Hz) ppm, respectively. The carbon atoms of C≡N, C–3, C–4, C–5, C–6 and C=S of pyridine moiety in compound **25** were resonated in its ^{13}C-NMR spectrum at δ 113.4, 45.9, 123.4, 124.2, 155.5 and 183.1 ppm, respectively.

Finally, we have succeeded to synthesize some novel fused pyran systems that would expect to have good biological properties. Thus, heating of the chromone derivative **3** with four examples of cyclic carbon nucleophiles namely, dimedone, 3-phenyl-1,4-dihydro-5*H*-pyrazol-5-one, barbituric acid and thiobarbituric acid in ethanolic sodium ethoxide for 10–12 hours afforded the corresponding fused pyran derivatives **26–29**, respectively (Scheme 10).[26] A plausible mechanism for the formation of the products **26–29** is depicted in Scheme 11. Initially, a nucleophilic attack of activated cyclic CH$_2$ at the position C–2 of chromone ring formed the intermediate **E**. The

Table 1 The in *vitro* cytotoxic effects of the synthesized compounds **3–29** against MCF-7, HEPG-2 and SKOV-3 cancerous cell lines[a]

Compounds	IC$_{50}$ (µg mL^{-1})		
	MCF-7	HepG-2	SKOV-3
3	12.79 ± 0.41	17.91 ± 2.06	17.03 ± 1.38
4	11.11 ± 4.62	4.854 ± 1.79	7.656 ± 0.97
5	9.357 ± 0.95	8.186 ± 1.51	6.580 ± 1.42
6	25.13 ± 2.63	21.01 ± 2.05	65.43 ± 3.25
7	1.152 ± 0.17	0.061 ± 0.03	3.323 ± 0.95
8	58.41 ± 2.67	18.90 ± 1.45	26.48 ± 2.88
9	49.43 ± 3.25	17.34 ± 1.12	23.20 ± 0.89
10	34.11 ± 2.24	16.16 ± 1.24	21.08 ± 1.23
11	1.992 ± 0.19	17.01 ± 2.65	3.910 ± 1.57
12	0.738 ± 0.07	1.910 ± 0.06	0.578 ± 0.31
13	75.86 ± 3.35	31.45 ± 5.69	27.66 ± 3.69
14	21.76 ± 3.33	23.67 ± 1.74	18.57 ± 2.17
15	1.601 ± 0.22	2.975 ± 1.01	0.380 ± 0.19
16	6.101 ± 1.84	7.920 ± 2.43	7.514 ± 1.93
17	4.821 ± 1.09	4.921 ± 2.18	5.321 ± 1.35
18	8.314 ± 2.64	16.28 ± 0.56	7.278 ± 2.60
19	0.650 ± 0.24	1.158 ± 0.41	1.086 ± 0.27
20	4.191 ± 0.99	16.92 ± 3.83	4.541 ± 0.86
21	17.09 ± 2.54	23.24 ± 2.43	15.11 ± 1.94
22	1.423 ± 0.27	0.674 ± 0.23	0.540 ± 0.05
23	10.37 ± 1.18	6.055 ± 1.26	2.544 ± 0.13
24	11.01 ± 1.23	12.03 ± 1.69	15.62 ± 1.94
25	18.12 ± 2.71	22.13 ± 2.82	17.53 ± 2.47
26	4.645 ± 0.90	2.408 ± 0.42	0.832 ± 0.05
27	10.32 ± 1.11	13.66 ± 2.59	6.559 ± 1.57
28	2.882 ± 0.36	3.079 ± 0.41	1.262 ± 0.06
29	6.531 ± 2.24	8.103 ± 2.45	7.513 ± 2.17
Doxorubicin	1.923 ± 0.38	1.510 ± 0.31	1.823 ± 0.42

[a] IC$_{50}$ values are the mean ± SD of three separate experiments.

Paper

keto–enol tautomerism between the intermediates **E** and **F** facilitated the nucleophilic attack of OH group on C=O of the active methyl compound, followed by elimination of water to produce the new pyran ring (Scheme 11). The structures of these pyran derivatives were established from IR, MS and NMR spectral data (see ESI†).

Fig. 1 Apoptosis/necrosis assessment for compounds **7**, **11**, **12**, **15**, **19**, **22**, **26** and **28** against MCF-7, subjected to previous treatment for 48 h, and apoptosis/necrosis quantified using flow cytometry. Data are presented as the mean ± SD; $n = 3$.

3. The cytotoxicity properties

3.1. Evaluation of cytotoxic effects

The in *vitro* cytotoxic effects of the novel synthesized compounds 3–29 were evaluated using the SRB assay against three cancer cell lines namely, human breast cancer cells (MCF-7), human liver cancer cells (HepG-2), and Human ovary cancer cells (SKOV-3) at doses ranging from 0.01 to 1000 µg.[27] The obtained results were compared with doxorubicin as standard anticancer drug. The results regarding cytotoxic activities are displayed as IC_{50} values in Table 1. Towards human breast cancer cells (MCF-7), compounds 7, 11, 12, 15, 17, 19, 20, 22, 26
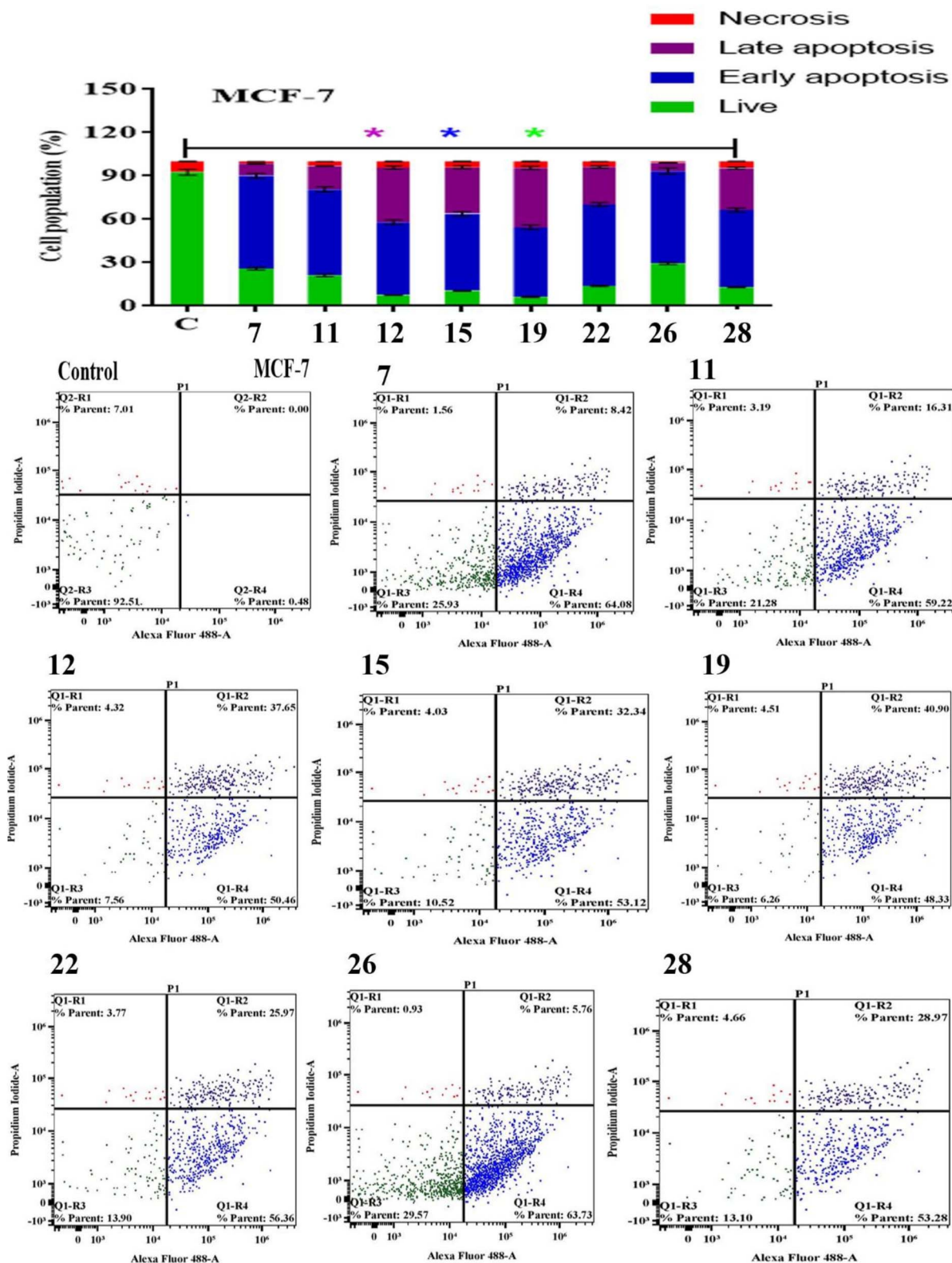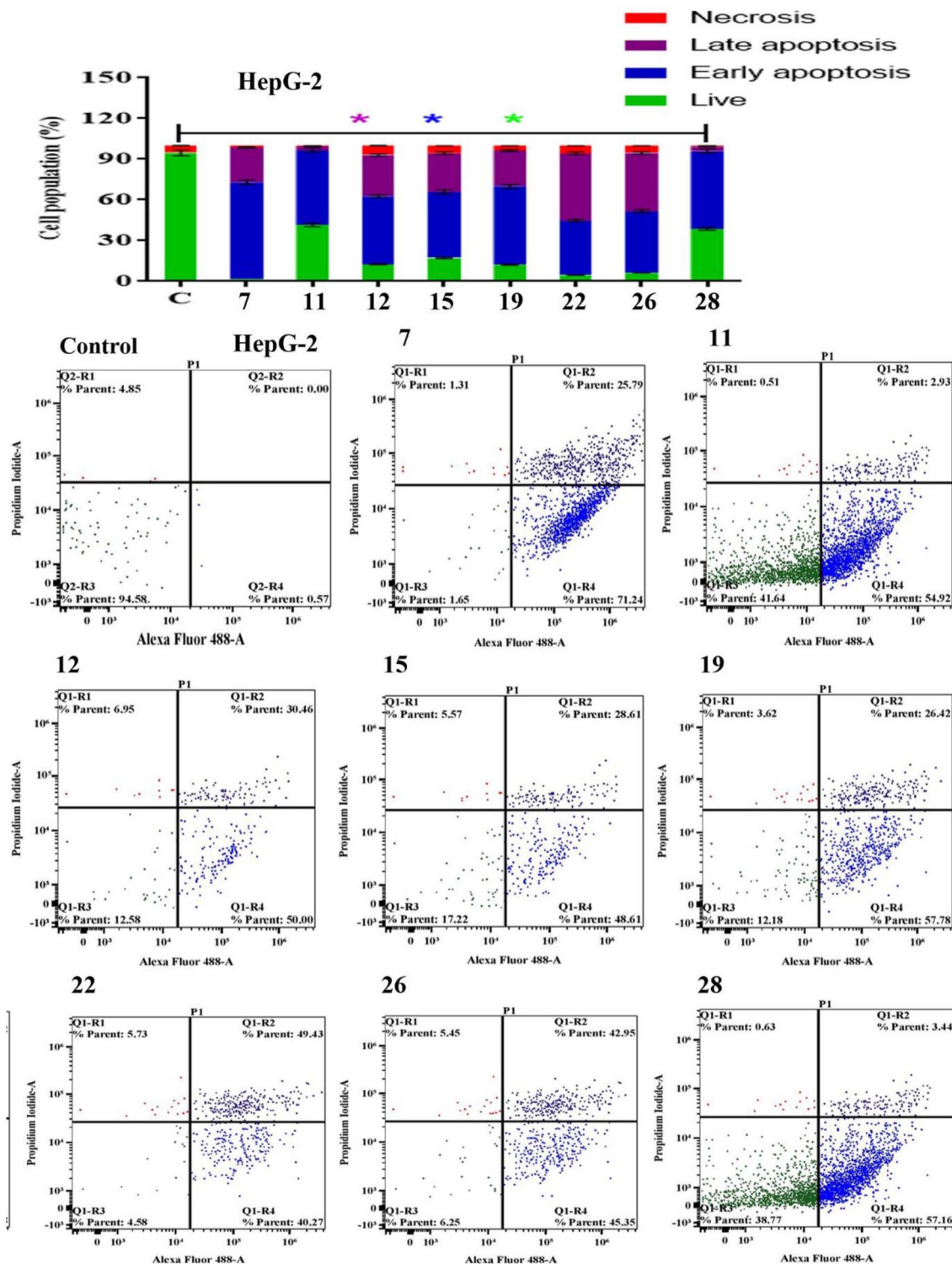

Fig. 2 Apoptosis/necrosis assessment for compounds 7, 11, 12, 15, 19, 22, 26 and 28 against HepG-2, subjected to previous treatment for 48 h, and apoptosis/necrosis quantified using flow cytometry. Data are presented as the mean ± SD; $n = 3$.

and **28** were the most promising candidates, exhibiting better cytotoxicity between IC$_{50}$ 0.650 ± 0.24 and 4.645 ± 0.90 µg ml^{-1}. In particular, compounds **7, 11, 12, 15, 19** and **22** were near or more active than doxorubicin (1.903 ± 0.38 µg ml^{-1}).[28] Further, the other compounds **4, 5, 16, 18, 23, 24, 27** and **29** showed moderate cytotoxicity, with IC$_{50}$ values in the range 6.101 ± 1.84 and 11.11 ± 4.62 µg ml^{-1}, while the remaining compounds exhibited low cytotoxicity on this cell line. With respect to human liver cancer cells (HepG-2), the compounds **4, 7, 12, 15, 17, 19, 22, 26** and **28** were found to be most potent in exerting
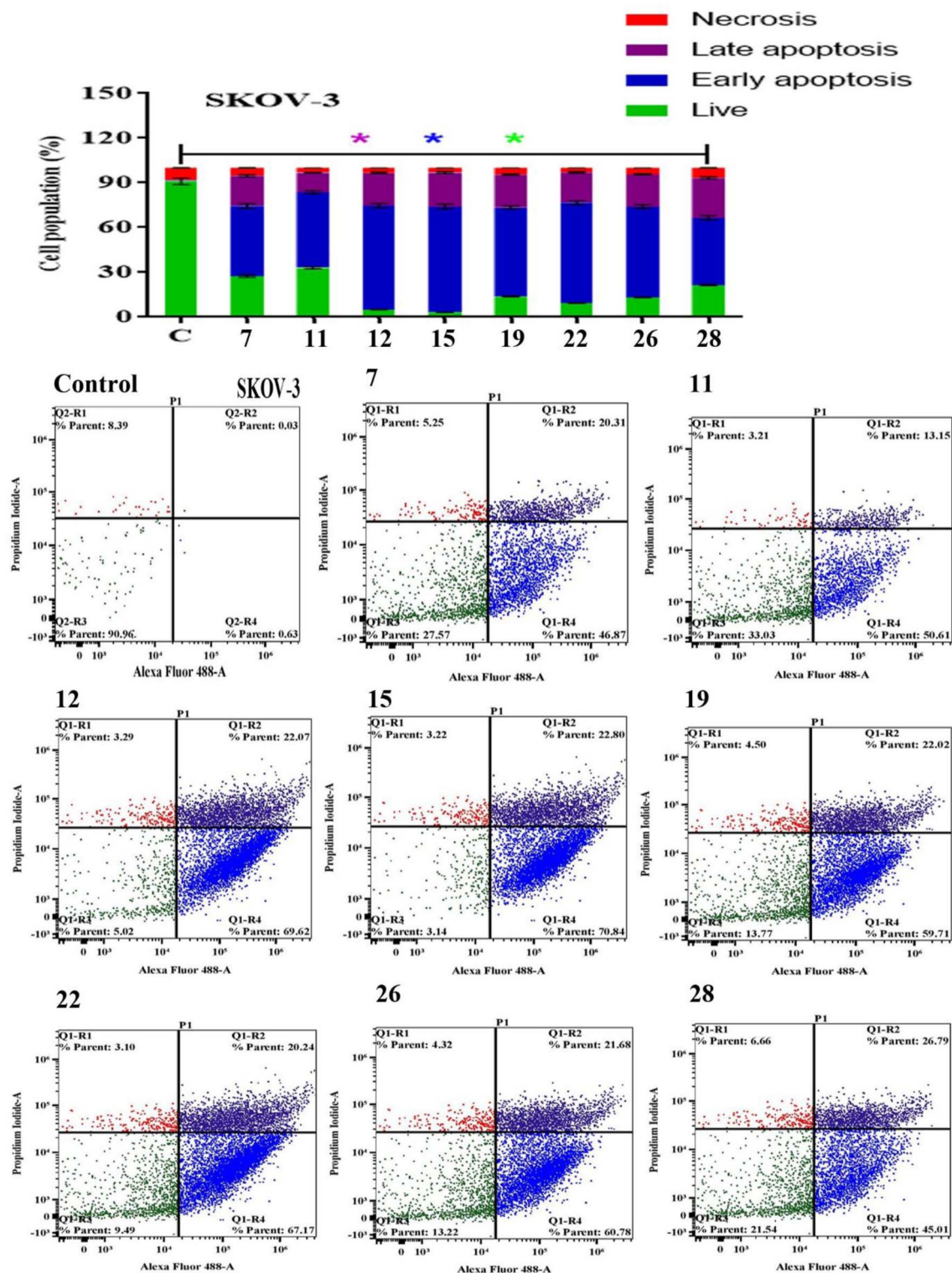

Fig. 3 Apoptosis/necrosis assessment for compounds **7, 11, 12, 15, 19, 22, 26** and **28** against SKOV-3, subjected to previous treatment for 48 h, and apoptosis/necrosis quantified using flow cytometry. Data are presented as the mean ± SD; $n = 3$.

cytotoxicity, with IC$_{50}$ values between 0.061 ± 0.03 and 4.854 ± 1.79 µg ml^{-1}. Especially, compounds **7, 12, 19** and **22** were more active than doxorubicin (1.501 ± 0.32 µg ml^{-1}).[29] In addition, compounds **5, 16, 23** and **29** were also sensitive towards HEPG-2 cancer cells with IC$_{50}$ between 6.055 ± 1.26 and 8.186 ± 1.51 µg ml^{-1}. On the other hand, the human ovary cancer cells (SKOV-3)

were easily killed by compounds **7, 11, 12, 15, 17, 19, 20, 22, 23, 26** and **29** which displayed their IC$_{50}$ values between 0.380 ± 0.19 and 4.541 ± 0.86 µg ml^{-1}. In particular, compounds **12, 15, 19, 22, 26** and **28** recorded better activities than doxorubicin (1.852 ± 0.42 µg ml^{-1}).[29] Moreover, compounds **4, 5, 16, 18, 27** and **29** were acceptable as potent agents (IC$_{50}$ values between

Fig. 4 The effect of compounds **7, 11, 12, 15, 19, 22, 26** and **28** on cell cycle distributions of MCF-7 cell lines. Cell cycle distribution was determined using DNA cytometry analysis after exposure to **7, 11, 12, 15, 19, 22, 26** and **28** for 48 h. Data are presented as the mean $\pm$ SD; $n = 3$; G1, G2 and S are cell cycle phases.

6.559 ± 1.57 and 7.656 ± 0.97 µg ml^{-1}) with respect to doxorubicin.

3.2. Structure activity relationship (SAR)

It was observed that cleavage of chromone ring and its closure into other heterocycles increased the cytotoxic effects which they compared with the substrate 3 and doxorubicin.

- The introducing of additional morpholine ring into the morpholinothiazolidinone as in both products 4 and 5 increased the cytotoxic effects.

- Generally, some pyrazole, pyrimidine and pyran derivatives bearing morpholino-thiazolidinone moiety displayed excellent cytotoxic effects depending on the nature of their substituents.

Fig. 5 The effect of compounds 7, 11, 12, 15, 19, 22, 26 and 28 on cell cycle distributions of HepG-2 cell lines. Cell cycle distribution was determined using DNA cytometry analysis after exposure to 7, 11, 12, 15, 19, 22, 26 and 28 for 48 h. Data are presented as the mean ± SD; $n = 3$; G1, G2 and S are cell cycle phases.

- The substitution of hydrogen atom of 1*H*-pyrazole ring in compound **6** by methyl group (product **7**) caused excellent cytotoxic effects towards all the three cancer cell lines.

- On the contrary, the *N*-aryl pyrazole **8–10** (Ar=C$_6$H$_5$, 4-NO$_2$C$_6$H$_4$ and 2,4-(NO$_2$)$_2$C$_6$H$_3$) did not improve the cytotoxic effects as in case of the *N*-methylpyrazole derivative **7**.

- The presence of nitro groups in both products **9** and **10** increased the cytotoxic effects when compared with compound **8**.

- The 2-amino- and 2-oxopyrimidine derivatives **12** and **15** displayed inhibition effects more than the 2-thioxo- and 2-selenoxopyrimidine derivatives **13** and **14**, respectively.
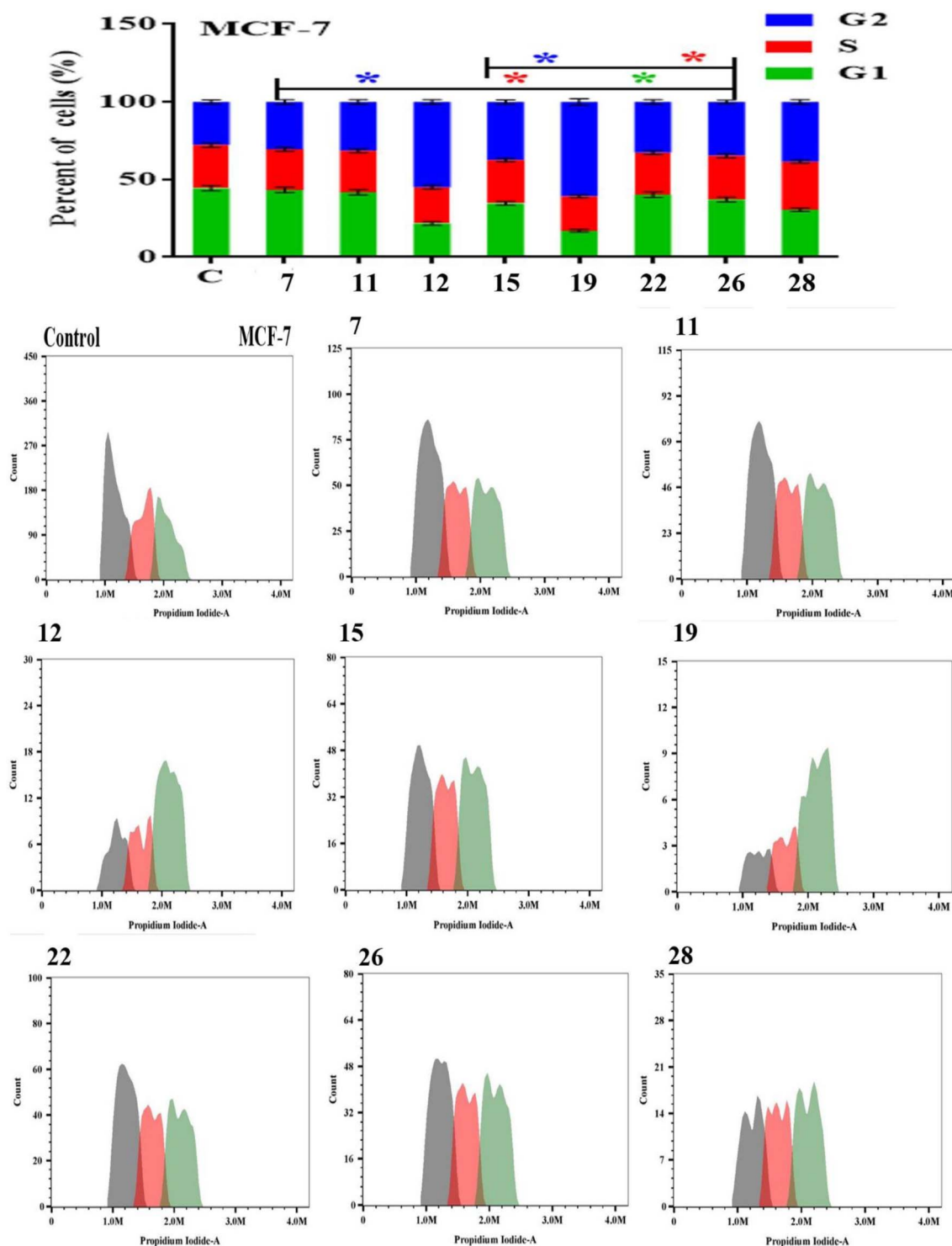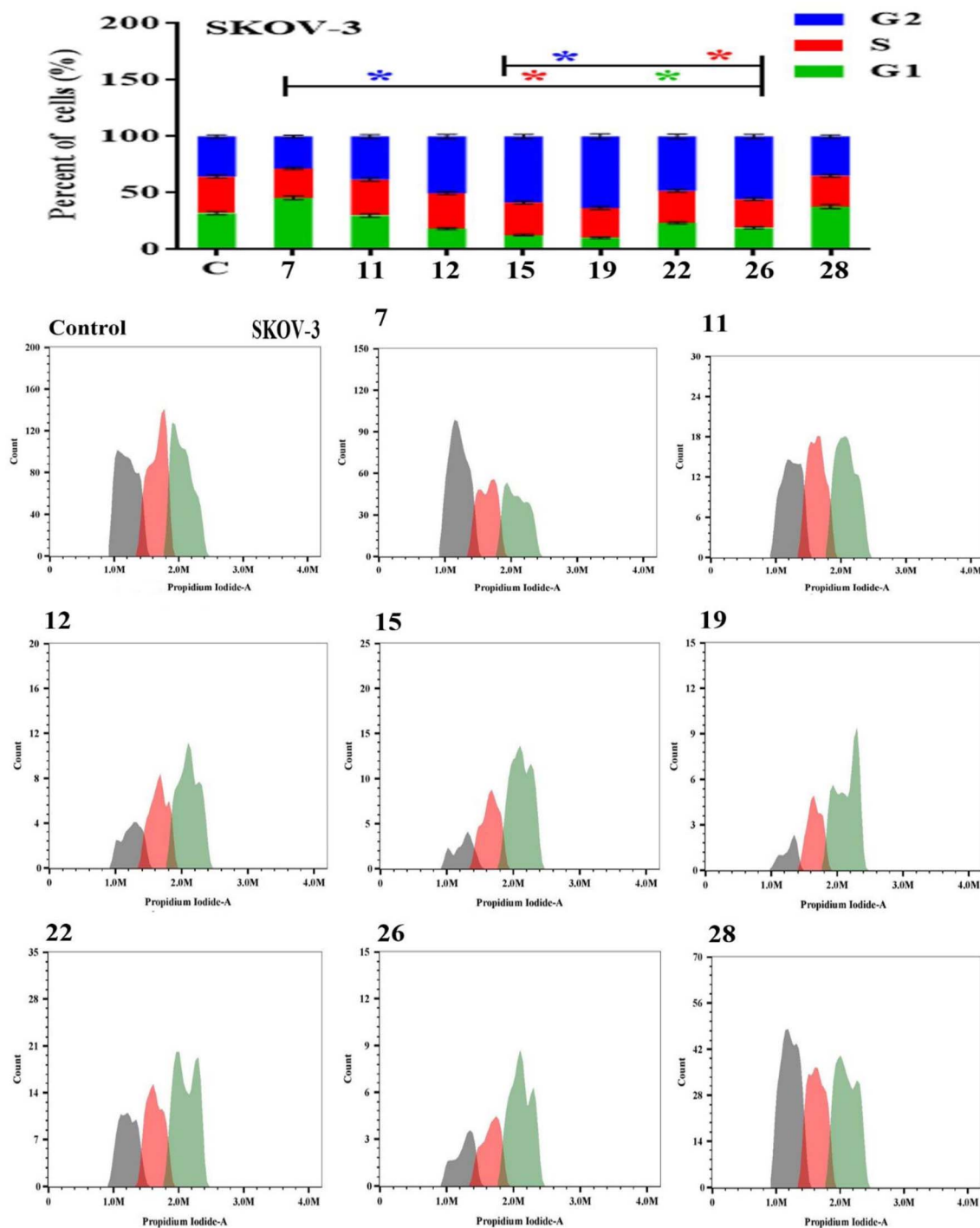

Fig. 6   The effect of compounds **7**, **11**, **12**, **15**, **19**, **22**, **26** and **28** on cell cycle distributions of SKOV-3 cell lines. Cell cycle distribution was determined using DNA cytometry analysis after exposure to **7**, **11**, **12**, **15**, **19**, **22**, **26** and **28** for 48 h. Data are presented as the mean ± SD; $n = 3$; G1, G2 and S are cell cycle phases.

- The fused pyrimidine systems such as midazopyrimidine **16** and triazolopyrimidine **17** displayed good cytotoxic properties.

- The conversion of chromone ring into seven-membered ring caused good cytotoxic properties especially, thiazepine **19** and diazepine **20** rings.

- The thiazepine ring **19** recorded inhibition effects more than diazepine and oxazepane.

- The presence of pyran moieties beard on the morpholino-thiazolidinone moiety (products **22**, **23**, **26–29**) fully succeed to increase the cytotoxic effects.

- The presence of imino group (C=NH) in pyran derivative **22** induced the cytotoxic effects more than the oxo group (C=O) in compound **23**.

- Interestingly, the fused pyran derivatives **26–29** recorded promising cytotoxic effects especially in both products **26**, **28** and **29**.

3.3. Apoptosis studies

Apoptosis evasion is a hallmark of the transformation of normal cells into tumor cells.[30] Common anticancer drugs aim to induce cell death through apoptosis; this is viewed as a requirement for blocking malignant cell growth.[31] The apoptotic cell death was caused by the promising compounds **7**, **11**, **12**, **15**, **19**, **22**, **26** and **28**. Alexa Fluor-488/PI staining was used to quantify the cells undergoing apoptosis by flow cytometry.[32] In MCF-7 cancer cell lines, the eight compounds strongly induced the early-apoptotic cell populations between 48.30–64.08%, while compounds **12**, **15**, **19**, **22** and **28** increased the late-apoptotic cell populations between 25.97–40.90%, in comparison with control cell (Fig. 1). With respect to HepG-2 cancer cell line, the eight compounds induced the early-

apoptotic cell populations to be between 40.27% and 71.24% while only compounds **7**, **12**, **15**, **19**, **22** and **26** increased the late-apoptotic cell populations in range 25.79–49.43% as depicted in Fig. 2. Interestingly, these eight compounds strongly increased the early-and late-apoptotic cell populations against SKOV-3 cell line in range 45.01–70.84% and 13.15–26.79%, respectively (Fig. 3). Finally, these eight compounds did not have any impacts in the necrotic assessment against the three cancer cell lines (Fig. 1–3).

3.4. Cell cycle studies

The Effect on the cell cycle distribution of solid tumor cells tracking tumor cell cycle phases was used to investigate the cytotoxic effects. As a result, the effect of the most promising compounds **7**, **11**, **12**, **15**, **19**, **22**, **26** and **28** were explored for cell cycle distribution to determine the intracellular mode of action of these compounds. The cells and vehicle control were treated with each precalculated IC_{50s} for 48 h, were stained with propidium iodide, and observed for cell cycle distribution by flow cytometry.[33] In MCF-7 cancer cell lines, the tested compounds did not significantly induce the cell distributions in the G1 and S phases in comparison with control cell. However, they strongly increased the cell distribution in the G2 phase to be between $30.53 \pm 1.40\%$ and $61.00 \pm 2.01\%$ (Fig. 4). These results showed that compounds **7**, **11**, **12**, **15**, **19**, **22**, **26** and **28** displayed acceptable arresting of the cell cycle in the G2 phase against MCF-7 cell lines. In the HepG-2 cells, only compounds **11**, **15**, **19** and **28** stopped these cells in the G1 phase between $37.92 \pm 1.50\%$ and $45.04 \pm 1.82\%$. In addition, the eight compounds except **7** did not cause a prominent increase in cell distribution in the S phase when compared with control. However, the G2 phase was increased to be in range $32.22 \pm 1.52\%$ and $52.14 \pm 1.94\%$ in the presence of all compounds except **15** and **19** (Fig. 5). As shown in Fig. 6, both compounds **7** and **28**-treated SKOV-3 cells increased the G1 phase to be $47.47 \pm 1.78\%$ and $37.79 \pm 1.65\%$, respectively, while the remaining compounds decreased the cell populations in this phase. Similarly, the eight compounds decreased of the cell distribution in the S phase compared to the control cells. On contrary, the same compounds except **7** and **28** showed an increase in the G2 phase to be between $38.17 \pm 1.63\%$ and $58.76 \pm 1.99\%$. These results showed that compounds **7** and **28** exhibited good arresting of the cell cycle in the G1 phase while compounds **15**, **19**, **22** and **26** were affected in the G2 phase against SKOV-3 cancer cell lines.

3.5. Molecular docking study

Molecular docking study was conducted to determine the suitable mechanism of cytotoxicity activities for the bioactive compounds **12** and **22**. The binding modes of the synthesized compounds to Mouse Double Minute 2 homolog (MDM2) (PDB ID: 4j3e) was studied. The inhibition of p53-MDM2 protein–protein interaction results in p53 accumulation and restore its tumor suppressor activity in cancer cells expressing wild-type p53. Blocking MDM2 to restore p53 function is a hotspot in the development of anticancer candidates.[34] The MDM2 was

Table 2 The interactions of compounds **12**, **22** and **Nutlin-3a** with MDM2 (4j3e)

Compound	Binding affinity (kcal mol^{-1})	Amino acid	Interaction types	Distance (Å)
12	−8.0	LEU 50	Pi–alkyl	5.43
		LEU 53	Pi–alkyl	4.88
		GLN 55	Hydrogen bond	2.96
		ILE 95	Pi–alkyl	4.50
		HIS 92	Hydrogen bond	3.19
		MET 58	Pi–Sulfur	5.43
		VAL 89	Pi–Sigma	3.96
22	−7.7	LEU 50	Pi–Alkyl	5.37
		LEU 53	Pi–Alkyl	5.21
		GLN 55	Hydrogen bond	3.16
		ILE 95	Pi–Alkyl	4.67
		HIS 92	Van der Waals	—
		MET 58	Pi–Sulfur	3.89
		GLN 68	Hydrogen bond	2.93
Nutlin-3a	−9.2	LEU 53	Pi–Alkyl	3.94
		GLN 55	Hydrogen bond	3.18
		ILE 95	Pi–alkyl	3.86
		LEU 50	Pi–alkyl	4.31
		HIS 92	Pi–Pi stacked	4.07
		MET 58	Pi–alkyl	4.92
		VAL 89	Pi–sigma	3.82

chosen as the target for docking studies because both compounds **12** and **22** recorded excellent cytotoxic effects against SKOV-3 and MCF-3 cell lines. It is known that MDM2 is highly expressed and correlated with the stages of the breast and ovarian cancer patients.[34] Nutlins are known as a class of potent and specific small molecule antagonists of p53-MDM2 inhibitors.[35] The Molecular docking was performed using Auto Dock Tools version 1.5.6 in 2D and 3D images.[36–41]

The binding affinity (kcal mol⁻¹) and the detailed interactions of **Nutlin-3a** and the synthesized compounds **12** and **22** were depicted in Table 2. As shown in Fig. 7, the binding mode of **Nutlin-3a** as co-crystalized ligand (affinity value of −9.2 kcal mol⁻¹) showed hydrogen bond with amino acid GLN

55. In addition, there were pi interactions including pi-alkyl (LEU 53, ILE 95, LEU 50 and MET 58), pi-sigma (VAL 89) and pi–pi T shaped (HIS 92) through planar aromatic regions with these amino acids (Fig. 7 and Supplemental Material).

The docking of compounds **12** and **22** with MDM2 (PDB ID: 4j3e) revealed that these compounds can form very similar interactions to that of the potent MDM2 antagonist **Nutlin-3a**.[42] Both products **12** and **22** showed similar binding mood with binding affinity of −8.0 and −7.7 kcal mol⁻¹, respectively. Products **12** and **22** formed pi-alkyl interactions through phenyl ring attached to *N*-thiazolidinone moiety with key residue LEU 50, LEU 53 and ILE 95 (Table 2). Moreover, weak pi–sulfur interactions were observed between pyran or pyrimidine
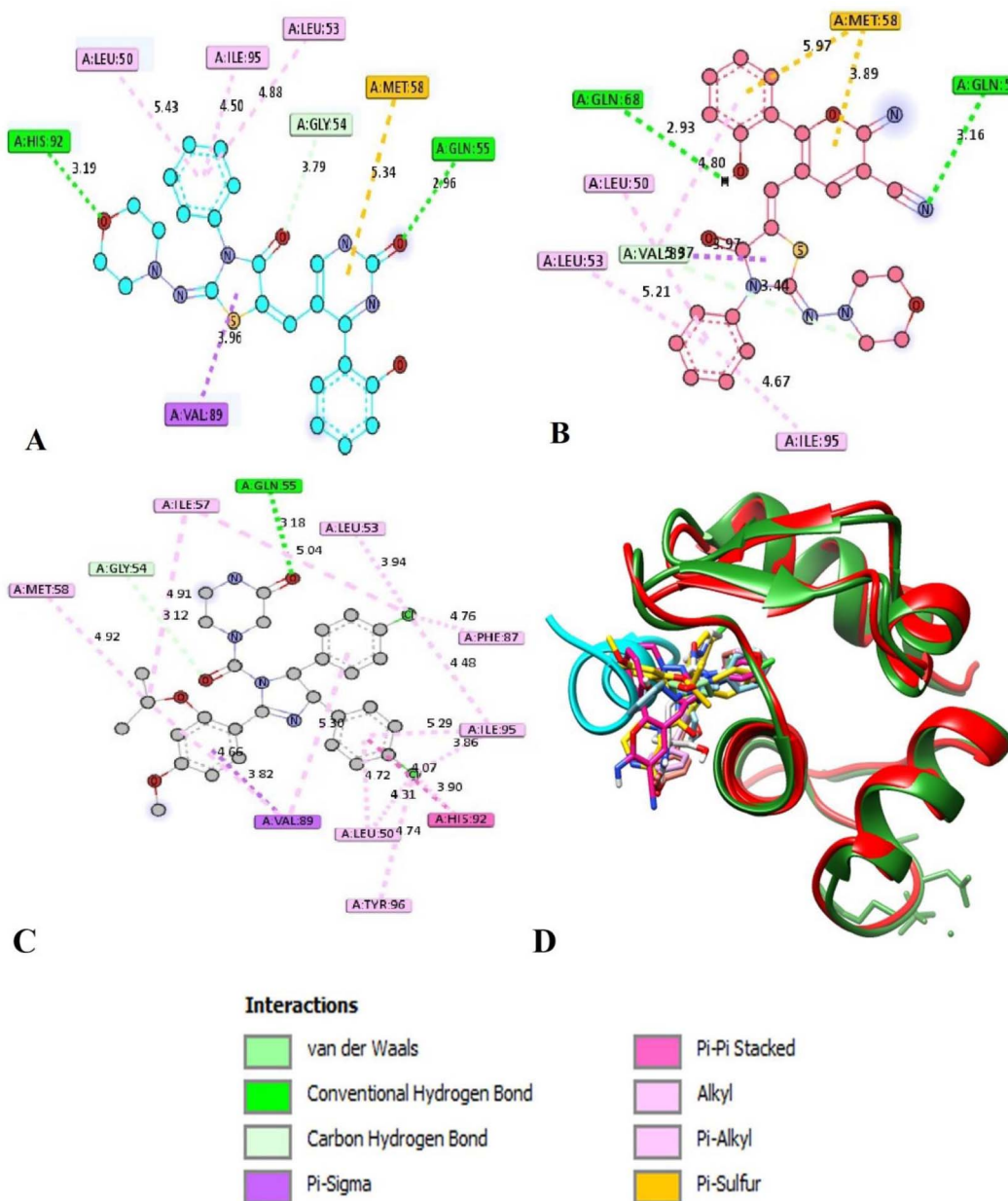

Fig. 7 Interactions of product **12** (A), **22** (B), **Nutlin-3a** (C) and all the studied compounds with **Nutlin-3a** occupying the same binding site of the natural ligand P53 (D).

© 2023 The Author(s). Published by the Royal Society of Chemistry

moieties and amino acid MET 58. Interestingly, both compound **12** and **22** can formed two extra interaction such as hydrogen bond between oxygen or nitrogen atoms of (O, C=O, OH, N≡C) and key amino acids HIS 92, GLN 55 and GLN 68. Compound **12** formed further pi-sigma interaction with amino acid VAL 89 (Table 2). Although both compounds **12** and **22** make two H-bonds in comparison with **Nutlin-3a**, their effects are less because of the overall binding energies are less than **Nutlin-3a**. Because of MDM2 can inhibit p53 activity by binding of its N-terminal domain to the *trans*-activation domain of p53 with the stages of the breast and ovarian cancer patients,[43] both compounds may be promising anti-metastatic ovarian cancer.

4. Conclusion

In this work, conversion of 2-(morpholinoimino)-5-[(4-oxo-4*H*-chromen-3-yl) methylene]-3-phenylthiazolidin-4-one (**3**) into a novel series of different nitrogen and oxygen heterocycles, was achieved by its reaction with different nitrogen and carbon nucleophiles. The analytical and spectral data evidenced the structure of newly designed derivatives. The in *vitro* cytotoxic activities of all synthesized derivatives were evaluated against MCF-7, HepG-2 and SKOV-3 cancerous cell lines. The synthesized derivatives **7**, **11**, **12**, **15**, **19** and **22** exhibited promising potency with IC$_{50}$ values ranging between IC$_{50}$ 0.650 ± 0.24 and 1.992 ± 0.19 μg ml^{-1} against MCF-7 cell which were near or more active than doxorubicin (1.903 ± 0.38 μg ml^{-1}). In addition, compounds **7**, **12**, **19** and **22** displayed their IC$_{50}$ values between 0.061 ± 0.03 1.910 ± 0.06 μg ml^{-1} against HepG-2 cell which were more active than doxorubicin (IC$_{50}$ at 1.501 ± 0.32 μg ml^{-1}). Further, compounds **12**, **15**, **19**, **22**, **26** and **28** recorded better activities than doxorubicin (IC$_{50}$ 1.852 ± 0.42 μg ml^{-1}) against SKOV-3 cell. Apoptosis was determined using flow cytometry along with cell cycle analysis and supported by a molecular docking. The products **7**, **11**, **12**, **15**, **19**, **22**, **26** and **28** induced a significant early-and late-apoptotic effect against all tumor cells while these products preferred to arrest all cancer cells in the G1 and G2 phases. Finally, the molecular docking studies were performed for compounds **12** and **22**, and the results indicated a negative binding energy with a similar or close to binding mode as described for the **Nutlin-3a** as co-crystalized inside the active sites of p53-MDM2 protein receptor.

Author contributions

Data curation: AAS and AAS. Formal analysis: AAS and AAS. Investigation: TEA, MNA, MYA and SEIE. Writing–original draft: TEA, MAA and MNA. Conceptualization: TEA, MAA and MNA. Supervision: TEA. Resources: TEA, MNA and SEIE. Software: TEA and SEIE. Methodology: MNA and SEIE. Writing – review & editing: TEA, MAA, MNA and SEIE. All authors read and approved the final version of the manuscript.

Conflicts of interest

Authors declare that they have no conflict of interest.

Acknowledgements

References

1 M. T. Gabr, N. S. El-Gohary, E. R. El-Bendary and M. M. El-Kerdawy, Synthesis and *in Vitro* Antitumor Activity of New Series of Benzothiazole and Pyrimido[2,1-*b*] Benzothiazole Derivatives, *Eur. J. Med. Chem.*, 2014, **85**, 576–592.

2 P. Kumar, M. Bhatt and A. Jha, Design, Synthesis and Anticancer Evaluation of Oxa/Thiadiazolylhydrazones of Barbituric and Thiobarbituric Acid: A Collective *in Vitro* and *in Silico* Approach, *ChemistrySelect*, 2018, **3**, 7060–7065.

3 W. Hanefeld and V. Helfri, Nitrosations of Hydrazine Derivatives, XI': 5-Nitrorhodanines from 5-Monosubstituted Rhodanine Derivatives under Nitrosating Conditions, *Arch. Pharm.*, 1993, **326**, 875–878.

4 J. A. War, S. K. Srivastava and S. D. Srivastava, Design, synthesis and molecular docking studies of some morpholine linked thiazolidinone hybrid molecules, *Eur. J. Chem.*, 2016, **7**, 271–279.

5 S. P. Vartale, Y. D. Pawar, N. K. Halikar and N. D. Kalyankar, DMAP as a versatile and highly efficient catalyst for N-acylation and N-sulphonation of substituted indole, *Int. J. Chem. Pharm. Sci.*, 2011, **2**, 50–56.

6 A. M. Al-Soliemy, T. A. Farghaly, E. M. H. Abbas, M. R. Shaaban, M. E. M. Zayed and T. B. A. El-Naggar, Synthesis of Thiazolyl-N-phenylmorpholine Derivatives and their Biological Activities, *Med. Chem.*, 2021, **17**, 790–805.

7 A. E. M. Mekky, S. M. H. Sanad and T. T. El-Idreesy, New thiazole and thiazole-chromene hybrids possessing morpholine units: Piperazine-mediated one-pot synthesis of potential acetylcholinesterase inhibitors, *Synth. Commun.*, 2021, **51**, 3332–3344.

8 K. Özadali, F. Özkanli, D. Erol, A. E. Dogan and K. Erol, Synthesis and Biological Activities of Some Thiazolidin-4-ones, *Arzneim.-Forsch./Drug Res.*, 2006, **56**, 678–681.

9 M. Lu, Y. Qi, Y. Han, Q. Yi, L. Xu, W. Sun, G. Ni, X. Ni and C. Xu, Design and development of novel thiazolidin-4-one-1,3,5-triazine derivatives as neuro-protective agent against cerebral ischemia reperfusion injury in mice *via* attenuation of NF-kb, *Chem. Biol. Drug Des.*, 2020, **96**, 1315–1327.

10 V. Y. Sosnovskikh, V. S. Moshkin and M. I. Kodess, Reactions of 3-(polyfluoroacyl) chromones with hydroxylamine: Synthesis of novel RF-containing isoxazole and chromone derivatives, *Tetrahedron*, 2008, **64**, 7877–7889.

11 A. S. Plaskon, O. O. Grygorenko and S. V. Ryabukhin, Recyclizations of 3-formyl-chromones with binucleophiles, *Tetrahedron*, 2012, **68**, 2743–2757.

12 T. E. Ali, M. A. Assiri, A. Y. Alzahrani, M. A. Salem, A. A. Shati, M. Y. Alfaifi and S. E. I. Elbehairi, An Effective Green One-Pot Synthesis of Some Novel 5-(Thiophene-2-Carbonyl)-6-

(Trifluoromethyl)Pyrano[2,3-c]Pyrazoles and 6-(Thiophene-2-Carbonyl)-7-(Trifluoromethyl)Pyrano[2,3-d]Pyrimidines Bearing Chromone Ring as Anticancer Agents, *Synth. Commun.*, 2021, **51**, 3267–3276.

13 T. E. Ali, M. A. Assiri, A. A. Shati, M. Y. Alfaifi and S. E. I. Elbehairi, Facile Green One-Pot Synthesis and Antiproliferative Activities of Some Novel Functionalized 4-(4-Oxo-4H-Chromen-3-yl)-Pyrano[2,3-c]Pyrazoles and 5-(4-Oxo-4H-Chromen-3-yl)Pyrano[2,3-d]Pyrimidines, *Russ. J. Org. Chem.*, 2022, **58**, 106–113.

14 T. E. Ali, M. A. Assiri, A. A. Shati, M. Y. Alfaifi and S. E. I. Elbehairi, One-pot three-component synthesis of a series of 2-amino-4-(4-oxo-4H-chromen-3-yl)-5-(2,2,2-trifluoroacetyl)-6-(trifluoromethyl)-4H-pyrans and 2-amino-4-(4-oxo-4H-chromen-3-yl)-5-(thiophene-2-carbonyl)-6-(trifluoromethyl)-4H-pyrans as promising anticancer agents, *Russ. J. Org. Chem.*, 2022, **58**, 584–591.

15 D. A. Bakhotmah, T. E. Ali, M. A. Assiri and I. S. Yahia, Synthesis of some novel 2-{pyrano[2,3-c]pyrazoles-4-ylidene}malononitrile fused with pyrazole, pyridine, pyrimidine, diazepine, chromone, pyrano[2,3-c]pyrazole and pyrano[2,3-d]pyrimidine systems as anticancer agents, *Polycyclic Aromat. Compd.*, 2022, **42**, 2136–2150.

16 M. A. Ibrahim and A. M. El-Kazak, Ring Opening and Recyclization Reactions with Chromone-3-carbonitrile, *J. Heterocycl. Chem.*, 2019, **56**, 1075–1085.

17 R. Navari, S. Balalaie, S. Mehrparvar, F. Darvish, F. Rominger, F. Hamdan and S. Mirzaie, Efficient synthesis of pyrazolopyridines containing a chromane backbone through domino reaction, *Beilstein J. Org. Chem.*, 2019, **15**, 874–880.

18 T. E. Ali, S. A. Abdel-Aziz, S. M. El-Edfawy, A. M. El-Hossain and S. M. Abdel-Kariem, Synthesis and biological evaluations of a series of novel azolyl, azinyl, pyranyl, chromonyl and azepinyl phosphonates, *Heterocycles*, 2013, **87**, 2513–2532.

19 B. L. Nilsson and L. E. Overman, Concise Synthesis of Guanidine-Containing Heterocycles Using the Biginelli Reaction, *J. Org. Chem.*, 2006, **71**, 7706–7714.

20 O. N. Petrova, L. L. Zamigajlo, K. S. Ostras, S. V. Shishkina, O. V. Shishkin, A. V. Borisov, V. I. Musatov, M. G. Shirobokova and V. V. Lipson, Multicomponent Reaction of 2-amino-benzimidazole, Arylglyoxals, and 1,3-cyclohexanedione, *Chem. Heterocycl. Compd.*, 2015, **51**, 310–319.

21 X. H. Liu, Y. M. Jia, B. A. Song, Z. X. Pang and S. Yang, Design and synthesis of novel 2-methyl-4,5-substituted benzo[f]-3,3a,4,5-tetrahydro-pyrazolo[1,5-d][1,4]oxazepin-8(7H)-one derivatives as telomerase inhibitors, *Bioorg. Med. Chem. Lett.*, 2013, **23**, 720–723.

22 M. Xie, R. K. Ujjinamatada, M. Sadowska, R. G. Lapidus, M. J. Edelman and R. S. Hosmane, A novel, broad-spectrum anticancer compound containing the imidazo[4,5-e][1,3]diazepine ring system, *Bioorg. Med. Chem. Lett.*, 2010, **20**, 4386–4389.

23 A. Moure, M. Orzlez, M. Sancho and A. Messeguer, Synthesis of enantiomerically pure perhydro-1,4-diazepine-2,5-dione and 1,4-piperazine-2,5-dione derivatives exhibiting potent activity as apoptosis inhibitors, *Bioorg. Med. Chem. Lett.*, 2012, **22**, 7097–7099.

24 M. A. Ibrahim and T. E. Ali, Ring opening and ring closure reactions of chromone-3-carboxylic acid: unexpected routes to synthesize functionalized benzoxocinones and heteroannulated pyranochromenes, *Turk. J. Chem.*, 2015, **39**, 412–425.

25 S. Kasmi-Mir, A. Djafri, L. Paquin, J. Hamelin and M. Rahmouni, One-Pot Synthesis of 5-Arylidene-2-Imino-4-Thiazolidinones under Microwave Irradiation, *Molecules*, 2006, **11**, 597–602.

26 R. Gasparová and M. Lácová, Reactions of 3-formylchromone with active methylene and methyl compounds and some subsequent reactions of the resulting condensation products, *Molecules*, 2005, **10**, 937–960.

27 A. M. Mahmoud, A. M. Al-Abd, D. A. Lightfoot and H. A. El-Shemy, Anticancer characteristics of mevinolin against three different solid tumor cell lines was not solely p53-dependent, *J. Enzyme Inhib. Med. Chem.*, 2012, **27**, 673–679.

28 H. A. Allam, M. E. Albakry, W. R. Mahmoud, A. Bonardi, S. A. Moussa, S. Mohamady, H. A. Abdel-Aziz, C. T. Supuran and H. S. Ibrahim, Effect of hydrophobic extension of aryl enaminones and pyrazole-linked compounds combined with sulphonamide, sulfaguanidine, or carboxylic acid functionalities on carbonic anhydrase inhibitory potency and selectivity, *Enzyme Inhib. Med. Chem.*, 2023, **38**, 2201403.

29 M. R. Elmorsy, E. Abdel-Latif, H. E. Gaffer, S. E. Mahmoud and A. A. Fadda, Anticancer evaluation and molecular docking of new pyridopyrazolotriazine and pyridopyrazolo-triazole derivatives, *Sci. Rep.*, 2023, **13**, 2782.

30 D. Hanahan and R. A. Weinberg, Hallmarks of cancer: the next generation, *Cell*, 2011, **144**, 646–674.

31 S. W. Fesik, Promoting apoptosis as a strategy for cancer drug discovery, *Nat. Rev. Cancer*, 2005, **5**, 876–885.

32 H. A. Bashmail, A. A. Alamoudi, A. Noorwali, G. A. Hegazy, G. Ajabnoor, H. Choudhry and A. M. Al-Abd, Thymoquinone synergizes gemcitabine anti-breast cancer activity *via* modulating its apoptotic and autophagic activities, *Sci. Rep.*, 2018, **8**, 11674–11685.

33 Z. A. Stewart, M. D. Westfall and J. A. Pietenpol, Cell-cycle dysregulation and anticancer therapy, *Trends Pharmacol. Sci.*, 2003, **24**, 139–145.

34 Y. Zhao, A. Aguilar, D. Bernard and S. Wang, Small-molecule inhibitors of the MDM2-p53 protein-protein interaction (MDM2 inhibitors) in clinical trials for cancer treatment, *J. Med. Chem.*, 2014, **58**, 1038–1052.

35 L. T. Vassilev, B. T. Vu, B. Graves, D. Carvajal, F. Podlaski, Z. Filipovic, N. Kong, U. Kammlott, C. Lukacs, C. Klein, N. Fotouhi and E. A. Liu, In Vivo Activation of the p53 Pathway by Small Molecule Antagonists of MDM2, *Science*, 2004, **303**, 844–848.

36 G. M. Morris, D. S. Goodsell, R. S. Halliday, R. Huey, W. E. Hart, R. K. Belew and A. J. Olson, Automated docking using a Lamarckian genetic algorithm and an

empirical binding free energy function, *J. Comput. Chem.*, 1998, **19**, 1639–1662.

37 R. Huey, G. M. Morris, A. J. Olson and D. S. Goodsell, A semiempirical free energy force field with charge-based desolvation, *J. Comput. Chem.*, 2007, **28**, 1145–1152.

38 G. M. Morris, R. Huey, W. Lindstrom, M. F. Sanner, R. K. Belew, D. S. Goodsell and A. J. Olson, AutoDock4 and AutoDockTools4: automated docking with selective receptor flexibility, *J. Comput. Chem.*, 2009, **30**, 2785–2791.

39 O. Trott and A. J. Olson, AutoDock Vina: improving the speed and accuracy of docking with a new scoring function, efficient optimization, and multithreading, *J. Comput. Chem.*, 2010, **31**, 455–461.

40 J. Eberhardt, D. Santos-Martins, A. F. Tillack and S. Forli, AutoDock Vina 1.2.0: New Docking Methods, Expanded Force Field, and Python Bindings, *J. Chem. Inf. Model.*, 2021, **61**, 3891–3898.

41 E. F. Pettersen, T. D. Goddard, C. C. Huang, G. S. Couch, D. M. Greenblatt, E. C. Meng and T. E. Ferrin, UCSF Chimera-A visualization system for exploratory research and analysis, *J. Comput. Chem.*, 2004, **25**, 1605–1612.

42 H. Zhu, H. Gao, Y. Ji, Q. Zhou, Z. Du, L. Tian, Y. Jiang, K. Yao and Z. Zhou, Targeting p53–MDM2 interaction by small-molecule inhibitors: learning from MDM2 inhibitors in clinical trials, *J. Hematol. Oncol.*, 2022, **15**, 91–95.

43 Y. Chen, D.-D. Wang, Y.-P. Wu, D. Su, T.-Y. Zhou, R.-H. Gai, Y.-Y. Fu, L. Zheng, Q.-J. He, H. Zhu and B. Yang, MDM2 promotes epithelial-mesenchymal transition and metastasis of ovarian cancer SKOV3 cells, *Br. J. Cancer*, 2017, **117**, 1192–1201.